

Femtosecond mode-locking and soliton molecule generation based on a GaAs saturable absorber

Chen-Yan Zhang(张辰妍), Xin-He Dou(窦鑫河), Zhen Chen(陈震), Jing-Han Zhao(赵靖涵), Wei Sun(孙薇), Ze-Yu Fan(樊泽宇), Tao Zhang(张涛), Hao Teng(滕浩), and Zhi-Guo Lv(吕志国)

Citation: Chin. Phys. B, 2025, 34 (**1**): 014205. DOI: 10.1088/1674-1056/ad8db3
Journal homepage: http://cpb.iphy.ac.cn; http://iopscience.iop.org/cpb

What follows is a list of articles you may be interested in

Nonlinear optical properties in n-type quadruple *δ*-doped GaAs quantum wells

Humberto Noverola-Gamas, Luis Manuel Gaggero-Sager, and Outmane Oubram
Chin. Phys. B, 2022, 31 (**4**): 044203. DOI: 10.1088/1674-1056/ac248e

Improved thermal property of strained InGaAlAs/AlGaAs quantum wells for 808-nm vertical cavity surface emitting lasers

Zhuang-Zhuang Zhao(赵壮壮), Meng Xun(荀孟), Guan-Zhong Pan(潘冠中), Yun Sun(孙昀), Jing-Tao Zhou(周静涛), and De-Xin Wu(吴德馨)
Chin. Phys. B, 2022, 31 (**3**): 034208. DOI: 10.1088/1674-1056/ac16d0

GaSb-based type-I quantum well cascade diode lasers emitting at nearly 2-μm wavelength with digitally grown AlGaAsSb gradient layers

Yi Zhang(张一), Cheng-Ao Yang(杨成奥), Jin-Ming Shang(尚金铭), Yi-Hang Chen(陈益航), Tian-Fang Wang(王天放), Yu Zhang(张宇), Ying-Qiang Xu(徐应强), Bing Liu(刘冰), and Zhi-Chuan Niu(牛智川)
Chin. Phys. B, 2021, 30 (**9**): 094204. DOI: 10.1088/1674-1056/abe930

Interlayer distance effects on absorption coefficient and refraction index change in p-type double-*δ*-doped GaAs quantum wells

H Noverola-Gamas, L M Gaggero-Sager, O Oubram
Chin. Phys. B, 2019, 28 (**12**): 124207. DOI: 10.1088/1674-1056/ab5278

Mid-infrared supercontinuum generation and its application on all-optical quantization with different input pulses

Yan Li(李妍), Xinzhu Sang(桑新柱)
Chin. Phys. B, 2019, 28 (**5**): 054206. DOI: 10.1088/1674-1056/28/5/054206

Femtosecond mode-locking and soliton molecule generation based on a GaAs saturable absorber

Chen-Yan Zhang(张辰妍)[1,†], Xin-He Dou(窦鑫河)[1,†], Zhen Chen(陈震)[1], Jing-Han Zhao(赵靖涵)[1], Wei Sun(孙薇)[1], Ze-Yu Fan(樊泽宇)[1], Tao Zhang(张涛)[1], Hao Teng(滕浩)[2], and Zhi-Guo Lv(吕志国)[1,‡]

[1] *School of Physical Science and Technology, Inner Mongolia University, Hohhot* 010021, *China*

[2] *Beijing National Laboratory for Condensed Matter Physics, Institute of Physics, Chinese Academy of Sciences, Beijing* 100190, *China*

(Received 24 September 2024; revised manuscript received 20 October 2024; accepted manuscript online 1 November 2024)

In the last few years, research on advanced ultrafast photonic devices has attracted great interest from laser physicists. As a semiconductor material with excellent nonlinear saturation absorption characteristics, GaAs has been used in solid-state and fiber lasers as a mode-locker. However, the pulse widths that have been reported in the searchable published literature are all long and the shortest is tens of picoseconds. Femtosecond pulse widths, desired for a variety of applications, have not yet been reported in GaAs-based pulsed lasers. In this work, we further explore the nonlinear characteristics of GaAs that has been magnetron sputtered onto the surface of a tapered fiber and its application in the generation of femtosecond lasing via effective dispersion optimization and nonlinearity management. With the enhanced interaction between evanescent waves and GaAs nanosheets, mode-locked soliton pulses as short as 830 fs are generated at repetition rates of 4.64 MHz. As far as we know, this is the first time that femtosecond-level pulses have been generated with a GaAs-based saturable absorber. In addition, soliton molecules, including in the dual-pulse state, are also realized under stronger pumping. This work demonstrates that GaAs-based photonic devices have good application prospects in effective polymorphous ultrashort pulsed laser generation.

Keywords: GaAs, saturable absorber, mode-locking, soliton molecule

PACS: 42.55.Wd, 42.60.–v, 42.60.Fc, 42.60.Gd

DOI: 10.1088/1674-1056/ad8db3 **CSTR:** 32038.14.CPB.ad8db3

1. Introduction

Following graphene, two-dimensional (2D) materials have gained increasing attention due to their unique optical and electrical properties, such as high electron mobility, strong light–matter interactions and tunable bandgaps.[1–5] One significant research direction is the application of 2D materials as photonic modulation devices in ultrashort pulsed laser generation. Compared with bulk materials, 2D materials exhibit superior characteristics in some aspects,[6] such as a greater broadband response to light and much stronger nonlinear absorption. Many 2D materials, such as graphene,[7] carbon nanotubes (CNTs), topological insulators (TIs),[8] metal–organic frameworks (MOFs),[9] perovskite,[10] MXene,[11] transition metal dichalcogenides (TMDs)[12] and black phosphorus (BP),[13] have been successively utilized as saturable absorbers (SAs) in pulsed lasers. Figure 1 provides an overview of the research progress made in the field of mode-locked pulse generation.[14–19] According to the type of material making up the SA, these research results can be divided into graphene, BP, single-walled CNTs (SWCNTs), TMDs and TIs. It is evident that the pulse width is predominantly concentrated in the microsecond and nanosecond levels, with femtosecond mode-locked pulses being less frequently generated. These investigations provide a valuable reference for promoting the development of robust lasers with high efficiency, low maintenance and low cost. Numerous experiments have shown that SAs with 2D materials as modulation devices frequently demonstrate excellent light–matter interaction ability, represented by a large modulation depth,[20] making them mature optoelectronic devices.

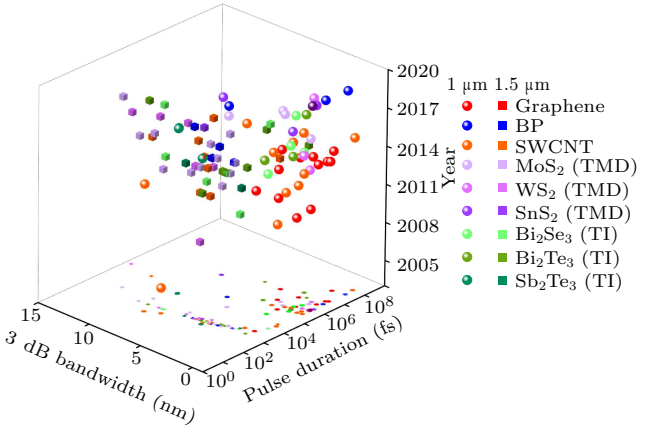


Fig. 1. Summary of research results on mode-locked fiber lasers based on novel 2D materials (BP, back phosphorus; SWCNT, single-walled carbon nanotube; TMD, transition metal dichalcogenide; TI, topological insulator).

As a second-generation semiconductor with a direct bandgap, gallium arsenide (GaAs) is recognized as one of the

†These authors contributed equally to this work.

‡Corresponding author. E-mail: lvzhiguo@imu.edu.cn

© 2025 Chinese Physical Society and IOP Publishing Ltd. All rights, including for text and data mining, AI training, and similar technologies, are reserved.

most promising materials for photonic devices, which benefit from its advantages in absorption rate, mobility and saturation drift velocity.[21–26] Consequently, its operational performance has been experimentally investigated for pulsed laser generation in both solid-state and fiber lasers.[27–31] However, for ultrafast lasers, one of the most critical specifications is the pulse width. There has been continuous exploration on how to generate laser pulses with a much shorter duration. In 1996, GaAs was applied in a solid-state Nd:YAG laser,[27] achieving nanosecond-level pulse outputs. Later, a pulse width as short as 24 ps was achieved in a Nd:YVO_4 laser.[28] Since then there have been no literature reports on the achievement of much shorter pulse widths with GaAs mode-locked solid-state lasers. One possible reason is that the laser field interacts directly with GaAs-based SAs, and the thermal damage to GaAs restricts the increase in intracavity average power in solid-state lasers,[32] leading to limited self-phase modulation (SPM) and the resulting narrower spectral broadening. In general, to acquire a shorter pulse width, effective dispersion management and nonlinear manipulation are also required during pulsed laser generation. In contrast to solid-state lasers, fiber lasers have advantages in dispersion compensation and nonlinear management. Moreover, the smaller core diameter can significantly enhance the nonlinear effects, typically self-phase modulation, thus exciting wider coherent spectral broadening and generating a narrower pulse width. Furthermore, fiber lasers also have more flexibility in terms of dispersion compensation, especially in the 1.5 μm waveband, because of the opposite sign dispersion in gain and passive fibers. In addition, special structures can be made with fibers so as to alleviate the thermal effect on materials with saturable absorption, such as tapered fibers. As the laser propagates along the lumbar area, the long-distance coupling between evanescent waves and SA material not only leads to an enhancement of the interaction intensity, but also strengthens the saturable absorption effect and releases the thermal load via indirect behavior. Up to now, only one work has been reported on a fiber laser based on GaAs as the SA, and the pulse width was 634 ps.[31] The inability to achieve a shorter pulse width may be primarily attributed to the uncompensated higher-order dispersion effects and nonlinear phase shifts that are induced by an excessively long laser cavity length (210 m). Therefore, it is crucial to effectively manage the intra-cavity dispersion and nonlinearity to achieve the desired femtosecond pulse performance. In conclusion, there have not yet been any reports on the realization of femtosecond pulse outputs in GaAs-based lasers, whether in solid-state lasers or fiber lasers. In fact, the shortening of pulse duration in ultrashort pulse lasers has consistently been a significant topic of investigation. Therefore, we believe that the potential of GaAs for use in ultrafast optical devices remains to be further exploited in femtosecond laser generation.

In this work, a GaAs magnetron sputtered on tapered fiber makes up the microfiber SA device, and generates a modulation depth of 5.51% and saturation intensity of 12.8 MW·cm^{-2}. Then the prepared SA is applied to an Er-doped fiber laser to realize femtosecond mode-locking. As far as we know, this is the first time that a GaAs-based laser has achieved femtosecond-level outputs. The 3 dB bandwidth, pulse width, repetition rate and signal to noise ratio (SNR) of the mode-locked pulses are measured to be 5.02 nm, 830 fs, 4.64 MHz and 80.5 dB, respectively. In addition, we can also achieve soliton molecules by increasing the pump power. The corresponding modulation period, pulse width (fitted by the sech^2 shape) and pulse interval are 0.83 nm, 1.73 ps and 9.20 ps, respectively. The results demonstrate that GaAs can serve as an excellent SA, possessing properties comparable to those currently reported for most 2D materials. This work indicates that GaAs can provide an effective means for ultrafast laser generation, which will expand the research and application prospects of 2D semiconductor materials in ultrafast optical device technology.

2. Preparation and characterization of SA material

Figure 2(a) shows the absorption spectrum of GaAs utilized in the experiment as measured by an ultraviolet–visible–near-infrared photodetector. The test range spans from 200 nm to 2000 nm. It can be seen that the maximum absorption peak is located at ∼ 980 nm. The absorption spectrum test for GaAs provides insights into its absorption characteristics at various wavelengths. By analyzing the absorption spectrum, we can determine the material's response to light at particular wavelengths, which directly affects its performance as an SA. Within the operational wavelength range of 976 nm it shows a high absorption rate, which can effectively suppress the high-order modes in lasers, thus facilitating stable mode-locking operation. To analyze the chemical and electronic states of the material, x-ray photoelectron spectroscopy (XPS) is employed.[33] Figure 2(b) presents the XPS survey spectrum of GaAs, where the electronic states corresponding to all peaks are labeled. Figure 2(c) depicts the XPS curve of As 3d, which can be further deconvoluted into two peaks at 44.4 eV and 41.1 eV, corresponding to As $3d_{3/2}$ and As $3d_{5/2}$, respectively, resulting from spin–orbit splitting. Figure 2(d) displays the XPS curve of Ga 3d, with an absorption peak at 20.0 eV. The lower-intensity peak located at 23.9 eV is the energy loss peak. XPS analysis reveals the chemical composition and surface state of GaAs. The XPS results inform us about the low degree of oxidation and fewer impurities present in GaAs, which may affect its electronic and nonlinear optical properties. A clean GaAs surface with a low oxidation level

is likely to exhibit superior nonlinear absorption characteristics, which are essential for efficient saturable absorption and mode-locking performance. Figure 2(e) shows an atomic force microscopy (AFM) image of GaAs, which characterizes the surface morphology. It can be observed that the GaAs coating is relatively uniform, with a thickness below 27.53 nm and primarily concentrated around 8.26 nm. The particles are evenly distributed with uniform sizes, meeting the requirements for the preparation of 2D materials. Figure 2(f) illustrates that the GaAs nanoparticles exhibit regular shapes, with no significant deviations in the thickness distribution curve, demonstrating a high degree of morphological consistency. AFM offers information about the surface morphology of GaAs, including its roughness and defect distribution. A smooth and uniform GaAs surface helps to reduce the scattering and loss of the beam during transmission. Additionally, AFM can also reveal the thickness and layering of GaAs, which are pivotal parameters affecting its nonlinear absorption characteristics and thermal management capabilities. These data indicate that GaAs can be fabricated into an SA for pulsed laser generation in subsequent experiments. Based on these characterization results, we can gain a comprehensive understanding of the physical and chemical properties of GaAs. These properties are the key to achieving high-performance SAs and stable mode-locked lasers. Under these favorable conditions, the modulation depth and recovery time of a GaAs SA are effectively enhanced, thereby promoting the establishment of ultrashort pulses and suppressing mode competition in lasers. These test results provide a solid foundation for the subsequent experiments and ensure the suitability of the design and the reliability of the experimental results.

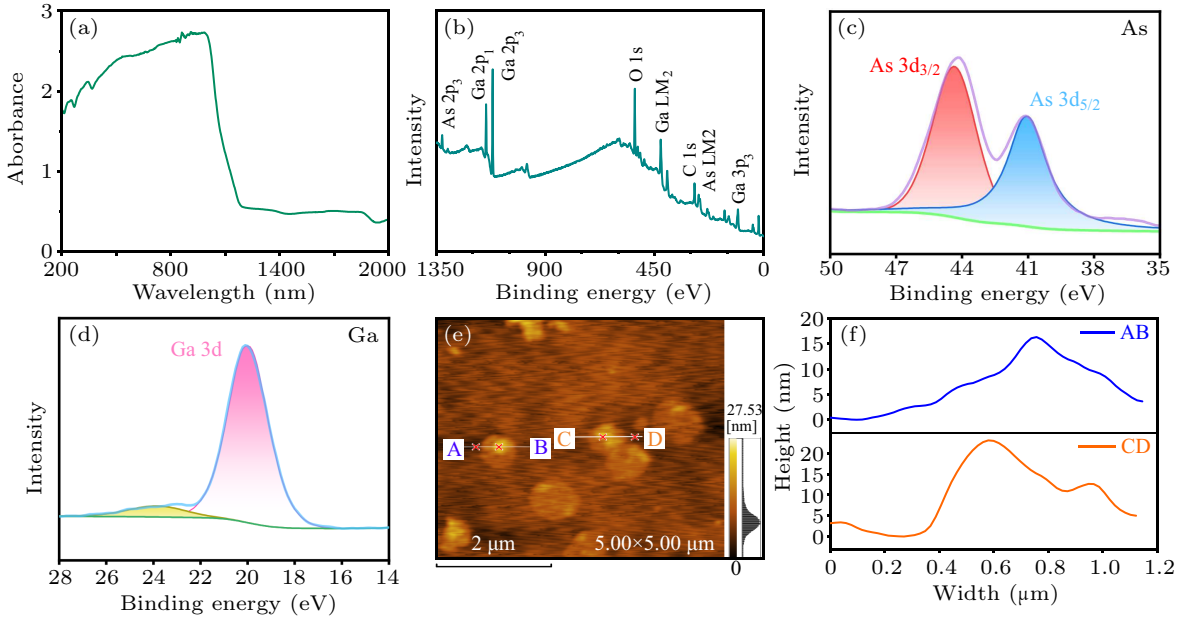


Fig. 2. Various material characterizations of GaAs: (a) absorption spectrum; (b) XPS survey spectrum of GaAs; (c) XPS spectrum for As 3d; (d) XPS spectrum for Ga 3d; (e) AFM image of GaAs; (f) thickness distribution curve of GaAs.

The prepared GaAs is uniformly coated onto the surface of a tapered fiber by magnetron sputtering, forming an SA. The coating process lasts for 8 min, during which helium gas is introduced into the chamber at a flow rate of 80 sccm and the sputtering instrument is operated at a power of 100 W. The nonlinear optical properties of the GaAs SA are measured by a home-made ultrashort pulsed laser source with a center wavelength of 1560.57 nm and a repetition rate of 11.95 MHz. The measured transmission curve is fitted with the typical saturation absorption formula[34]

$$T(I) = 1 - \alpha_0 \cdot \exp\left(-\frac{I}{I_{\text{sat}}}\right) - \alpha_{\text{ns}}, \tag{1}$$

where $T(I)$, α_0, α_{ns}, I and I_{sat} represent the transmittance, modulation depth, nonlinear loss, incident peak intensity and saturation intensity, respectively. The calculated modulation depth and saturation intensity are 5.51% and 12.8 MW·cm^{-2}, respectively, as shown in Fig. 3. It can be seen in the figure that the measured data basically fall into the 95% confidence band. Usually, the modulation depth of an SA is defined as the maximum change in transmission induced by the incident light. The low modulation depth may be attributed to the following two reasons. One is that the structure of the fiber is destroyed in the fused tapering process. The thin core disrupts the symmetry of the fiber and increases the transmission loss. However, the elongated cone region enhances the nonlinear interaction between GaAs and evanescent waves, thereby facilitating the generation of a pulsed laser, which is verified in the following experiment. The second factor might be associated with the phenomenon of two-photon absorption (TPA), which intensifies as the incident light intensity increases. TPA refers

to the process in which a medium absorbs or combines two photons of the same or different energies to excite electrons from low-energy states in the valence band to higher energy states. When the light intensity reaches a certain level, the material's absorption of light becomes saturated, and further increases in light intensity result in no change or minimal change in the absorption coefficient. Consequently, under intense illumination, there is a competitive relationship between TPA and saturable absorption. When the light intensity is sufficiently high, TPA may become significant, diminishing or masking the SA effect to some extent. In summary, the phenomenon of TPA can reduce the modulation depth of materials. However, TPA contributes to reducing the unnecessary modes within the laser cavity, thereby enhancing the stability of mode-locked pulses. Therefore, the introduction of a tapered fiber is generally beneficial to the formation and stabilization of a pulsed laser.

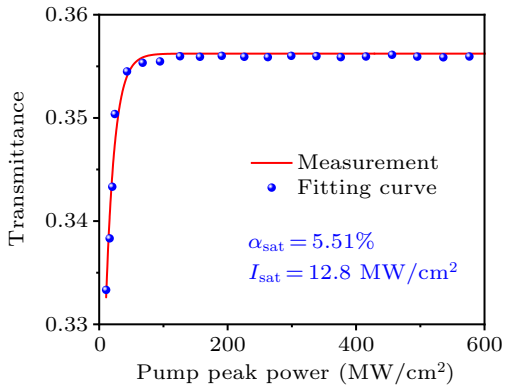


Fig. 3. Nonlinear optical transmission of the prepared GaAs SA.

3. Ultrafast laser applications

3.1. Experimental setup

The experimental setup utilized to explore the operational performance of GaAs as an SA in femtosecond laser generation is schematically shown in Fig. 4. In the cavity, the pump source is a 976 nm laser diode (LD), with a maximum output power of 400 mW, and a section of 60 cm gain fiber (Liekki Er110-4/125, with a dispersion of 0.012 $ps^2 \cdot m^{-1}$) is used as the gain medium. The gain fiber and pump light source are connected through a 980/1550 nm wavelength division multiplexer (WDM). In the experiment, a polarization-insensitive isolator (PI-ISO) is employed to guarantee unidirectional oscillation of the light. In the meantime its use ensures that the initiation of mode-locking depends solely on GaAs and eliminates the possibility of nonlinear polarization rotation. A polarization controller (PC) is placed within this cavity to optimize laser polarization and assist mode-locking activation. A 90:10 output coupler (OC) is employed to extract 10% of the laser power as an output. A section of single-mode fiber (SMF; SMF-28e, Corning) is inserted into the cavity to adjust the cavity dispersion. The total length and net dispersion of the cavity are 43.1 m and -0.9278 ps^2, respectively. The detecting instrument includes a 600 MHz oscilloscope (Tektronix, TBS1202C), 2 GHz InGaAs PIN detector (EOT, ET-3000), a 600–1700 nm spectrum analyzer (YOKOGAWA, AQ6370D), a 10 Hz–26.5 GHz radio-frequency (RF) spectrum analyzer (Kesight, N9010B) and a 100 fs–500 ps autocorrelator (A.P.E., SM2000).

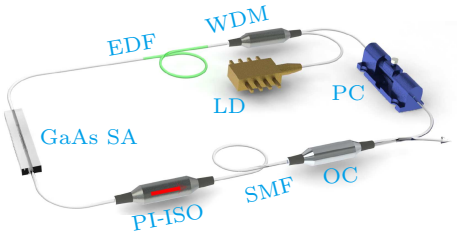


Fig. 4. Schematic diagram of the mode-locked fiber laser based on a GaAs SA (LD, 976 nm laser diode; WDM, wavelength division multiplexor; GaAs SA, GaAs-based saturable absorber; PI-ISO, polarization-independent isolator; EDF, erbium-doped fiber; PC, polarization controller; OC, output coupler; SMF, single-mode fiber).

3.2. Fundamental mode-locking operation

When the pump power exceeds 80 mW, a stable mode-locked pulse train can be observed on the oscilloscope (Tektronix, TBS1202C) by adjusting the PC. The pulse sequence of the mode-locked laser is shown in Fig. 5(a); its period is measured as 216 ns, which aligns with the round-trip time of the ring cavity. Figure 5(b) exhibits a spectrum with 0.1 nm resolution, the center wavelength is 1565 nm and the 3 dB spectrum width is about 5.02 nm. Symmetric Kelly sidebands can be observed on both sides of the central peak, which are caused by interference between dispersive waves and solitons, indicating that the solitons are generated in the negative dispersion region.[3] The reason for the appearance of Kerry sidebands is that the phase difference between them is a multiple of 2π, thus producing obvious interference between dispersive waves and solitons. As shown in Fig. 5(c), the fundamental repetition rate is 11.63 MHz, with a SNR up to 80.5 dB (with a 1 MHz span and 1 Hz resolution bandwidth). The inset in Fig. 5(c) shows the RF spectrum recorded in a 120 MHz long span with a resolution of 10 kHz. The results further demonstrate the stability of the proposed mode-locked fiber laser. An autocorrelation trace is illustrated in Fig. 5(d), which can be well fitted by a $sech^2$ curve. According to the fitting results, the pulse duration is about 830 fs. Then we replace the GaAs-based SA with a tapered fiber of the same length to confirm whether the mode-locking operation is purely induced by GaAs nanosheets. In this case, the mode-locking operation cannot be observed again, despite extensive tuning of the pump power and PC. Therefore, we conclude that the GaAs-based SA exhibits excellent saturable absorption characteristics, enabling it to function as an efficient mode-locker

to realize femtosecond mode-locking operation in EDF lasers.

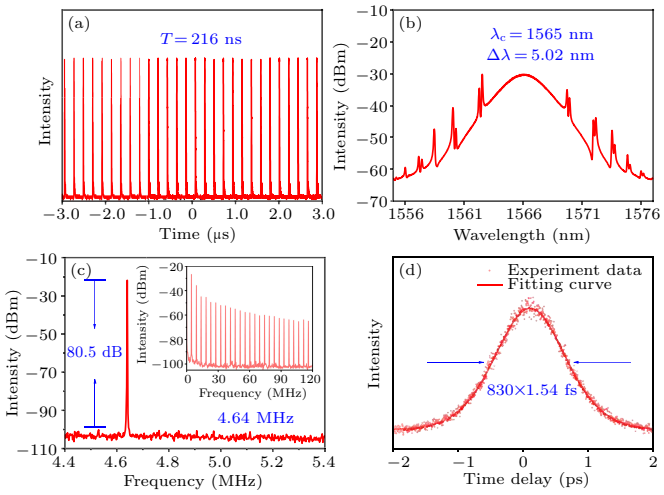


Fig. 5. Characteristics of mode-locked fiber lasers: (a) mode-locked pulse sequences; (b) spectrum of the laser; (c) RF spectrum near the fundamental frequency and RF spectrum within 120 MHz span; (d) autocorrelation trace and the corresponding sech^2 fitting curve.

3.3. Soliton molecule operation

In the anomalous dispersion regime, the natural balance between nonlinearity and dispersion, gain and loss can contribute to the formation of optical solitons. However, when the disturbance within the laser cavity becomes excessively large, the equilibrium may be disrupted, resulting in alterations to the pulse characteristics. Bound solitons are two or more fundamental solitons tightly bound together in the temporal or spatial domain through direct interaction. They are valuable in lasers for generating stable, high-intensity ultrashort pulses. By reducing the pump power (100 mW), the laser can enter bound-state soliton mode-locking. This may be because the gain decreases concomitantly with the pump power, which leads to the destruction of the balance in the cavity and the inability to stabilize the pulse through the gain, resulting in pulse splitting. In general, the soliton molecule manifests with a modulated spectrum and autocorrelation trace,[35] as shown in Fig. 6. Figure 6(a) illustrates the mode-locked spectrum of the soliton molecule, which is centered at 1565 nm, with a 0.83 nm spatial period. Moreover, a symmetrical second maximum peak can be observed, indicating a π-phase-locked bound state.[2] There is an obvious Kelly sideband in the spectrum, which results from the interference fringes of the two closely spaced solitons. Figure 6(b) is the corresponding autocorrelation trace, revealing a triple-peaked structure. The time separation between these adjacent lateral peaks is 9.20 ps, and the pulse width of the central peak is 1.73 ps assuming a sech^2 pulse shape, which matches the modulation period of the spectrum (this can be calculated by the Fourier transformation formula $c\Delta T\Delta\lambda = \lambda_0^2$).[36] At the same time, the pulse time interval is about 5.32 times the pulse duration, which indicates the generation of loosely bound soliton pairs. The different peaks in the autocorrelation trace have an intensity ratio of 1:2:1, which indicates the existence of secondary modulations in the detailed spectrum.[37]

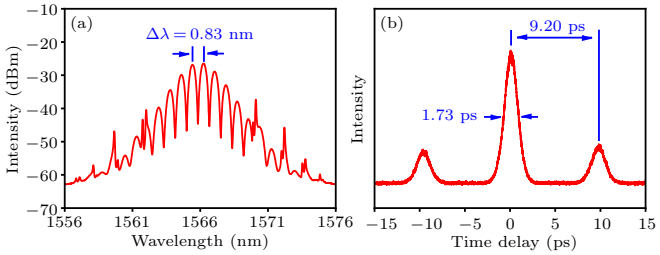


Fig. 6. Soliton molecule characteristics: (a) optical spectrum; (b) autocorrelation trace.

4. Conclusion

We know that dispersion and nonlinear effects are important parameters for high-quality ultrashort pulse generation. In this work, a GaAs-based SA is applied in a fiber laser and a pulse width at the femtosecond level has been realized for the first time via the enhanced nonlinear interactions between evanescent waves and GaAs without thermal damage to the fiber lumbar area in combination with effective dispersion management. In addition, dual-pulse soliton molecules can also be achieved, with the two pulses having the same duration of 1.73 ps and a time separation of 9.20 ps. The pulse widths, whether in fundamental mode-locking or soliton molecule operation, are all among the shortest in the reported literature. The results indicate that GaAs possesses comparable laser performance to most of the reported nanomaterials (graphene, CNTs, TIs, MOFs, MXene, TMDs etc.) and could be used as a promising SA for generation of ultrafast pulsed fiber lasers as long as effective techniques are utilized. We believe that this work enriches the research on nonlinear optical properties of GaAs and deepens our understanding of its ultrafast photonics.

Acknowledgements

Project supported by the National Natural Science Foundation of China (Grant No. 12164030), Young Science and Technology Talents of Inner Mongolia, China (Grant No. NJYT22101), the Central Government Guides Local Science, the Technology Development Fund Projects (Grant No. 2023ZY0005), and the Science and Technology Plan Projects of Inner Mongolia Autonomous Region of China (Grant No. 2023KYPT0012).

References

[1] Han Y, Guo Y, Gao B, Ma C, Zhang R and Zhang H 2020 *Prog. Quantum Electron.* **71** 100264

[2] Han Y, Gao B, Wen H, Ma C, Huo J, Li Y, Zhou L, Li Q, Wu G and Liu L 2024 *Light Sci. Appl.* **13** 101

[3] Li L, Xue Z, Pang L H, Xiao X S, Yang H R, Zhang J N, Zhang Y M, Zhao Q Y and Liu W J 2024 *Opt. Lett.* **49** 1293
[4] Li L R, Li X H, Zhao Y, Feng J J, Zhang C X C X, Shi Y, Ge Y Q and Zhang Y N 2022 *Nanotechnology* **33** 18
[5] Han Y H, Li X H, Chen E C, An M Q, Song Z Y, Huang X Z, Liu X F, Wang Y S and Zhao W 2022 *Adv. Opt. Mater.* **10** 2201034
[6] Wang G, Baker-Murray A A and Blau W J 2019 *Laser Photonics Rev.* **13** 1800282
[7] Bao Q L, Zhang H, Wang Y, Ni Z H, Yan Y L, Shen Z X, Loh K P and Tang D Y 2009 *Adv. Funct. Mater.* **19** 3077
[8] Zhao C, Zhang H, Qi X, Chen Y, Wang Z, Wen S and Tang D 2012 *Appl. Phys. Lett.* **101** 211106
[9] Sun Z H, Jiang X T, Wen Q, Li W J and Zhang H 2019 *J. Mater. Chem. C* **7** 4662
[10] Li P F, Chen Y, Yang T S, Wang Z Y, Lin H, Xu Y H and Li L 2017 *ACS Appl. Mater. Interfaces* **9** 12759
[11] Jiang X T, Li W J, Hai T, Yue R, Chen Z W, Lao C S, Ge Y Q, Xie G Q, Wen Q and Zhang H 2019 *NPJ 2D Mater. Appl.* **3** 34
[12] Wang S, Yu H, Zhang H, Wang A, Zhao M, Chen Y, Mei L and Wang J 2014 *Adv. Mater.* **26** 3538
[13] Sotor J, Sobon J, Kowalczyk M, Macherzynski W, Paletko P and Abramski K M 2015 *Opt. Lett.* **40** 3885
[14] Wang J L, Wang X L, Lei J J, Ma M Y, Wang C, Ge Y Q and Wei Z Y 2020 *Nanophotonics* **9** 2315
[15] Liu X M, Popa D and Akhmediev N 2019 *Phys. Rev. Lett.* **123** 093901
[16] Su X B, Shao F H, Hao H M, Liu H Q, Li S L, Dai D Y, Shang X J, Wang T F, Zhang Y, Yang C A, Xu Y Q, Ni H Q, Ding Y and Niu Z C 2023 *Chin. Phys. B* **32** 098103
[17] Xiao Y J, Xing X W, Cui W W, Chen Y Q, Zhou Q and Liu W J 2023 *Chin. Phys. B* **32** 054201
[18] Jiang T, Yin K, Wang C, You J, Ouyang H, Miao R L, Zhang C X, Wei K, Li H, Chen H T, hang R Y, Zheng X, Xu Z J, Cheng X G and Zhang H 2020 *Photonics Res.* **8** 78
[19] Novoselov K S, Geim A K, Morozov S V, Jiang D, Zhang Y S, Dubonos S V, Grigorieva I V and Firsov A A 2004 *Science* **306** 666
[20] Li L, Pang L, Zhao Q, Wang Y and Liu W 2020 *Nanophotonics* **9** 2569
[21] Paajaste J, Suomalainen S, Koskinen R, Härkönen A, Steinmeyer G and Guina M 2012 *Phys. Stat. Solid. C* **9** 294
[22] Liu X M and Pang M 2019 *Laser Photonics Rev.* **13** 1800333
[23] Ma H C, Wang Y X and Deng A P 2022 *Chin. Phys. B* **31** 010201
[24] Milovanov Y, Skryshevsky V, Gavrilchenko I, Oksanich A, Pritchin S and Kogdas M 2019 *J. Electron. Mater.* **48** 2587
[25] Lockwood D J, Schmuki P, Labbe H J and Fraser J W 1999 *Physica E* **4** 102
[26] Akinlami J O and Ashamu A O 2013 *JOS* **34** 032002
[27] Kajava T T and Gaeta A L 1996 *Opt. Lett.* **21** 1244
[28] Scurtescu C, Zhang Z Y, Alcock J, Fedosejevs R, Blumin M, Saveliev I, Yang S, Ruda H and Tsui Y Y 2007 *Appl. Phys. B: Lasers Opt.* **87** 671
[29] Li D C, Zhao S Z, Li G Q and Yang K J 2010 *Optik* **121** 478
[30] Li P, Wang Q P, Zhang X Y, Wang Y R, Li S C, He J L and Lu X Q 2001 *Opt. Laser Technol.* **33** 383
[31] Yang S, Yang Y Y, Zhang L, Huang J Y, Bai Y R and Lin X C 2019 *Optik* **178** 1218
[32] Li J, Pan Y B, Zeng Y P, Liu W B, Jiang B X and Guo J K 2013 *Int. J. Refract Met. H* **39** 44
[33] Engelhard M H, Lyubinetsky A and Baer D R 2016 *Surf. Sci. Spectra* **23** 83
[34] Du J, Wang Q K, Jiang G B, Xu C W, Zhao C J, Xiang Y J, Chen Y, Wen S C and Zhang H 2014 *Sci. Rep.* **4** 6346
[35] Olivier M and Piché M 2019 *Opt. Express* **17** 405
[36] Chen Z K, Zhou J and Zhao J Q 2023 *IEEE J. Quantum Electron.* **59** 1600207
[37] Liu R M, Wang T S, Ma W Z, Zhao D S, Lin P, Wang F R and Zhao Y W 2019 *IEEE Photonic Tech. Lett.* **31** 341